

1     **VARIANCE PROCESSING FOR STABLE BOUNDARY-LAYER HEIGHT ESTIMATION**  
2                     **USING BACKSCATTER LIDAR DATA: A DISCUSSION**

3                     *Muñoz-Porcar, C.<sup>1</sup>, Araujo da Silva, M.P.<sup>1</sup>, Saeed, U.<sup>2</sup>, Rey, F.<sup>3</sup>,*  
*Tanamachi, R.L.<sup>3</sup>, Pay, M.T.<sup>4</sup>, and Rocadenbosch, F.<sup>1,5</sup> Senior member, IEEE*

<sup>1</sup>CommSensLab-UPC, Department of Signal Theory and Communications (TSC),

Universitat Politècnica de Catalunya (UPC), Campus Nord, E-08034 Barcelona, Spain.

<sup>2</sup>Department of Communications and Networking, Aalto University, Espoo, 00076, Finland.

<sup>3</sup>Department of Signal Theory and Communications, UPC, Campus Nord, E-08034 Barcelona, Spain.

<sup>4</sup>Barcelona Supercomputing Center (BSC), Earth Sciences, E-08034, Barcelona, Spain

<sup>5</sup>Institute of Space Studies of Catalonia, IEEC, E-08034 Barcelona, Spain

4                     **ABSTRACT**

5     In this paper we present a method for estimating the height of the nocturnal stable boundary layer by using lidar measurements  
6     and a single radiosonde for unambiguous initial guess. The method relies on the correlation between aerosol stratifications in

---

This work was supported via Spanish Government–European Regional Development Funds project PGC2018-094132-B-I00 and EU H2020 ACTRIS-IMP (GA 871115). CommSensLab is a María-de-Maeztu Unit of Excellence funded by the Agencia Estatal de Investigación, Spain. The work of M.P. Araujo da Silva was supported by the Spanish Ministry of Science, Innovation and Universities under Grant PRE2018-086054. Data were provided by Jülich Observatory for Cloud Evolution (JOYCE-CF), a core facility funded by Deutsche Forschungsgemeinschaft via grant DFG LO 901/7-1.

7 the stable boundary layer and minimum variance levels in the attenuated backscatter profile. The method is based on calculating  
8 either temporal or spatial variance vertical profiles of the attenuated backscatter and threshold-limited decision. A radiosonde  
9 temperature-based estimation is used to provide an initial guess if several minimum variance regions are detected. Two study  
10 cases using ceilometer data are shown. Comparison with temperature-based estimations from a collocated microwave radiome-  
11 ter have been used for validation. The method can be useful for estimating the stable boundary layer height in sites with a  
12 ceilometer but without any available temperature profiler.

13 ***Index Terms***— Laser radar, remote sensing, signal processing, stable boundary layer.

## 14 1. INTRODUCTION

15 The Atmospheric Boundary Layer height (ABLH) is a key parameter in atmospheric science and air quality modelling. In  
16 spite of its importance, the ABLH cannot be directly measured and has to be estimated from the signature within the profiles  
17 of temperature, water vapor, aerosols, wind, and other trace gases [1]. Different types of measuring systems have been used  
18 for sensing the troposphere, including remote sensing instruments like microwave radiometers (MWR), sodar and lidar or in  
19 situ instruments hosted in weather balloons, radiosondes (RS) and aircrafts. Among them, ground-based lidars have widely  
20 been used for aerosols studies in the boundary layer. They are active instruments relying on the principle of laser radars, that  
21 is, they collect, detect and process light scattered by atmospheric aerosols and molecules when they are illuminated by laser  
22 radiation [2]. Networks of lidar systems such as EARLINET [3] and MPLNET [4] have been deployed during years to provide  
23 measurements over wide geographic areas and conditions. A typical ABL diurnal cycle over land for a clear convective day  
24 consists of a mixed layer (ML) during the daytime and a nighttime stable boundary layer (SBL) topped by a residual-layer (RL)  
25 [5]. The structure of the Nocturnal Boundary Layer (NBL) at a particular location and time depends upon different physical  
26 processes and it can be classified into fully turbulent (also known as nighttime ML), intermittently turbulent, and non-turbulent  
27 (which is the one known as SBL). The nocturnal SBL is characterized by multiple layers of aerosols spanning over the horizontal

28 dimension, with varying widths in the vertical dimension. In a previous work from the authors [6] it has been shown that the  
29 SBLH is correlated with both a minimum variance region (MVR) of the attenuated backscatter (a proxy of the backscatter  
30 coefficient for moderately-to-clear atmospheres) and temperature inversion from stable to neutral [5]. This approach combines  
31 ceilometer-based attenuated backscatter vertical profiles with MWR-based temperature ones by using an adaptive filter. In the  
32 present work, we introduce a derived work to estimate the SBLH from MVRs relying on ceilometer attenuated-backscatter data  
33 only and reference RS data. Alternatively to using coarse MWR-based SBLH estimates we use RS data for initialization and  
34 verification/control. The method is also based on temporal / spatial variance processing of the backscatter signal but does not  
35 make use of any adaptive filter to blend data from the two sensors. Two datasets of measurements provided by a ceilometer  
36 during two different representative atmospheric situations will be used to test the method. The results will be compared with  
37 SBLH estimates from MWR measurements.

## 38 2. INSTRUMENTS AND DATA-SET

39 The ceilometer used in this work is a Jenoptik CHM 15k Nimbus [7]. It has a transmission wavelength of 1064 nm and  
40 a temporal and spatial resolution of  $\Delta T = 15$  s and  $\Delta z = 15$  m, respectively. The MWR is a HATPRO (Humidity and  
41 Temperature Profiler) manufactured by Radiometer Physics GmbH (RPG), Germany. The dataset of measurements has been  
42 collected during the HD(CP)<sup>2</sup> Observational Prototype Experiment (HOPE) campaign (April 02 - July 24, 2013) at Jülich  
43 Observatory for Cloud Evolution (JOYCE). Overall, 226 RS (Graw, mod. DFM-09) were launched during the campaign,  
44 although most of them ( $\simeq 75\%$ ) were operated in daytime mixed-layer conditions. A single nocturnal RS was daily launched at  
45 23:00 UTC. Moreover, during Intensive Observations Periods (IOPs: 15/04, 18/04, 20/04, 24/04, 25/04, 29/04, 02/05, 04/05,  
46 05/05, and 18/05) several RS were also launched at different times during the night and early morning (21:00, 03:00, 05:00,  
47 07:00 and 09:00 UTC).

### 3. SBLH ESTIMATION USING VARIANCE PROCESSING AND BACKSCATTER LIDAR DATA

The method can be implemented using either temporal or spatial variance estimation. Fig. 1 shows the block-diagram of the temporal variance processing for identifying MVRs and, eventually, estimation of the SBLH. First, the ceilometer backscatter dataset is saved as a matrix,  $\beta(z, t)$ . Second, and to simplify discussion of the results, the backscatter profiles are height clustered. Then, the mean power spectrum density (PSD) of each backscatter time series is computed to assess the best moving-average (MA) window length in each cluster. This length is chosen so as to ensure a reasonable trade-off between time resolution and noise rejection. The third block computes, by using a MA rectangular window, the temporal variance matrix (TVAR =  $\hat{V}_\beta(z, t)$ ), which describes the time variance of the backscatter signal at each height. The last stage tackles MVRs identification. The processing steps for spatial variance processing follow similar steps and yield a spatial variance matrix (SVAR) containing the vertical variance profiles at each time instant with a height resolution defined by the spatial window length.

#### 3.1. Height and time clustering

Concerning temporal variance processing, the 24-h measurement dataset is clustered into three physically different height intervals: 360-644 m (nighttime SBL and daytime lowest ML), 1259-1543 m (daytime top of the ML and nighttime RL), and 1558-1993 m (free troposphere).

Similarly, spatial variance processing is carried out by first clustering the 24-h dataset into five time intervals: 00:00-05:00 UTC (early-morning SBL), 05:00-10:00 UTC (morning transition time), 10:00-16:00 UTC (daytime mixed-layer), 16:00-21:00 UTC (afternoon transition time), and 21:00-24:00 UTC (nighttime SBL). For space economy, only the temporal variance formulation will be presented next, the spatial one being essentially identical.

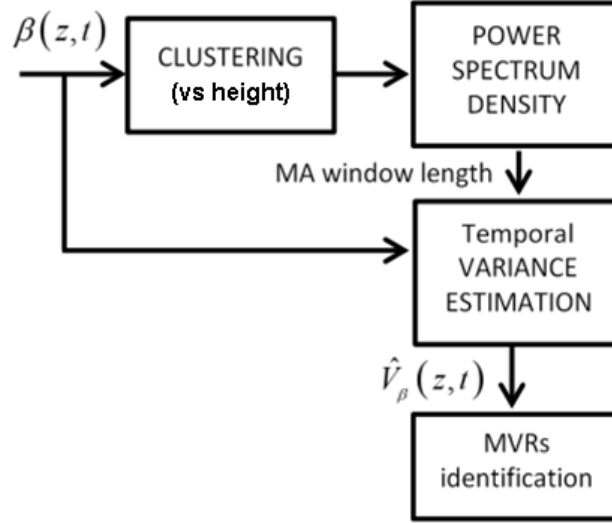


**Fig. 1.** Block diagram for SBLH estimation using temporal variance processing.

### 66 3.2. Estimation of the MA window length: Resolution

67 As a second step, the optimal length of the MA window is computed. Towards this end, the PSD of the representative profiles  
 68 in each cluster is calculated using the periodogram [8]. The PSD reveals signal and noise power distribution over the frequency  
 69 spectrum. It permits to identify the cut-off frequency where the signal becomes buried into noise, thus providing a MA window  
 70 length that ensures that significant backscatter variations are assimilated into the variance calculation. A minimum length of 6  
 71 samples is set to limit the error in the variance estimation (Eq. (1)). Regarding temporal processing, most of the signal power  
 72 in the three height clusters is concentrated in frequencies below  $f_{c,tmp} = 1.1$  mHz, which translates to a temporal resolution  
 73 window,  $w_{tmp} = 1/f_{c,tmp} = 909s \simeq 15$  min (60 samples).

### 74 3.3. MA variance processing of the backscatter signal

Once the best window length has been determined, the temporal variance matrix is computed from the backscatter at each height

$z_p, \beta_p(k) = \beta(t_k, z_p) = \beta(t_1, z_p), \dots, \beta(t_N, z_p)$ , where  $k$  is a reminder of discrete time and  $N$  is the number of time samples.

The temporal variance is estimated as [9]

$$\hat{Var}[\beta_p(k)] = \frac{1}{M} \sum_{i=k-(M-1)/2}^{k+(M-1)/2} [\beta_p(i) - \hat{\mu}_p^\beta(k)]^2; \quad (1)$$

where  $k = (M - 1)/2, \dots, N - (M - 1)/2$ .

75 In Eq. (1)  $M$  is the window length (in samples) and is the mean value of the backscatter within the MA window at each time,  
 76  $k$ . The temporal variance matrix is obtained by repeating the same calculation of Eq. (1) for each point  $p = 1 \dots P$  along the  
 77 height grid. The effective temporal resolution is computed as  $M\Delta T$ . The uncertainty associated to the variance estimation of  
 78 Eq. (1) is computed as the standard deviation of the estimation error. Formally, the uncertainty at height  $z = z_p$  as a function  
 79 of time instant  $k$  can be written as [9]

$$\sigma_p(k) = \sqrt{Var[y_p(k)]}; y_p(k) = \hat{Var}[\beta_p(k)]. \quad (2)$$

80 In practice, the variance of  $y_p(k)$  (i.e., the variance of the estimated backscatter variance) is computed in the same MA  
 81 fashion as Eq. (1) above.

82 Fig. 2 shows five vertical profiles of the temporal (green line) and spatial variances (blue line) at five representative times  
 83 (2:30, 7:30, 13:00, 18:30, 22:30 UTC, center time of of each time cluster) along with their respective errorbars. The vertical  
 84 profiles of both TVAR and SVAR methods agree well in all five panels. It can be noticed that deep and wide MVRs -as proxies  
 85 of SBLH stratification- only appear clearly during nighttime (e.g., from about 400 to 700 m and from 950 to 1200 m at 2:30  
 86 UTC and from 700 m to 1000 m at 22:30 UTC, see red arrows). On the other hand, the maximum variance (red ellipses) is  
 87 attained at the top of the ML during the daytime (at about 1300 m at 13:00 UTC) and coinciding with what likely is the RL  
 88 during the nighttime (1300 m at 2:30 UTC and 1100 m at 22:30 UTC).

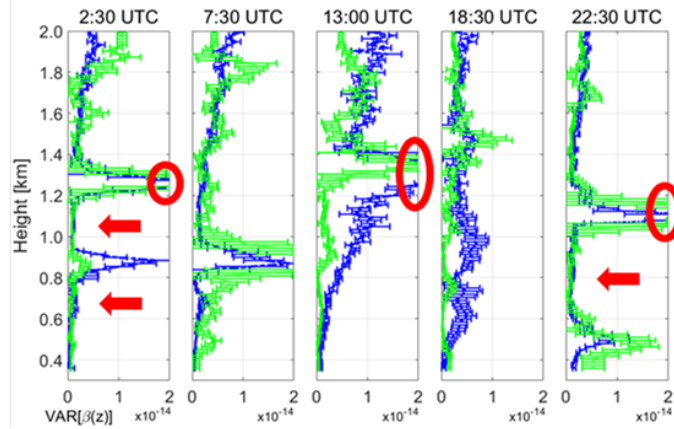


**Fig. 2.** Temporal (green line) and spatial (blue line) variance profile at 5 instant times. (Arrows) and (ellipses) indicate minimum and maximum variance regions, respectively. Local time is UTC + 1h.

### 89 3.4. MVRs identification

90 The first step towards SBLH estimation is to identify MVRs in the backscatter variance profiles of Fig. 2. Since the SBLH  
 91 is almost always lower than 1 km, the search for MVRs has been limited to the first km of the variance profile. MVR upper  
 92 and lower boundaries are defined by the intercept points where variance is greater than three times the estimated variance  
 93 uncertainty,  $\hat{Var}[\beta(z)] \geq 3\hat{\sigma}$ , where  $z$  is the minimum variance point of the MVR. Once one or several MVRs are identified  
 94 in a variance profile, the next step is to estimate the SBLH. In case of a single MVR, the SBLH is estimated as the height  
 95 corresponding to the absolute minimum of the variance in the MVR. SBLH total uncertainty is directly given by the width of  
 96 the MVR. In case of multiple MVRs, an initial guess for the SBLH is helped by the RS temperature-based estimate.

## 97 4. RESULTS AND DISCUSSION

98 Two study cases from the HOPE campaign have been considered to test the approach presented in Section 3: The first case,  
 99 24/04/2013, is a predominantly clear-sky day. Figs. 3(a)(b) show the backscatter colorplot along with SBLH estimates using  
 100 temporal and spatial variance processing for two time intervals (0-5 UTC and 21-24 UTC). The time resolution of the temporal  
 101 and spatial minimum-variance-based SBLH estimates are respectively 15 minutes (imposed by the MA window length) and

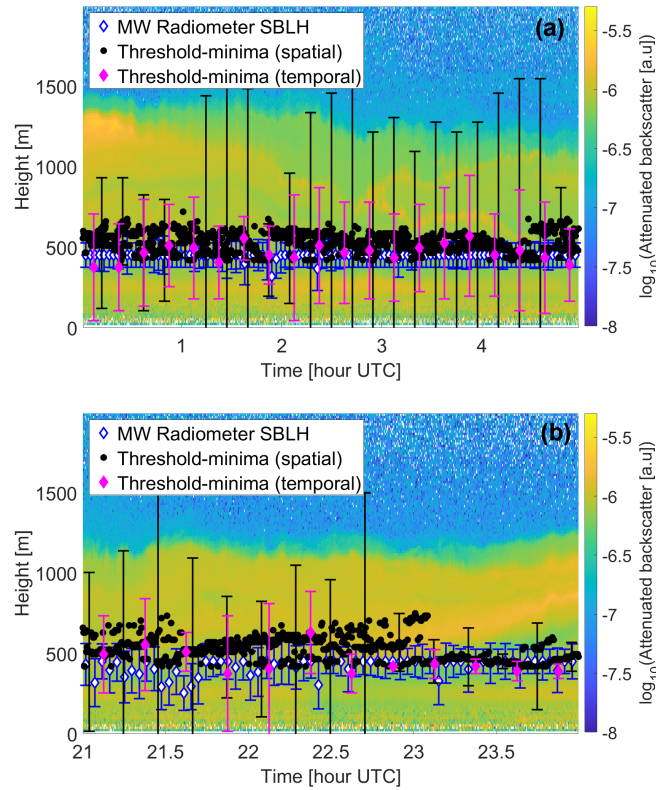


**Fig. 3.** Stable boundary layer height estimation in two time intervals (early morning (a) and night (b)) on 24/4/2013.

102 15 seconds (the one of the raw ceilometer data). The vertical resolution when using temporal and spatial processing are,  
 103 respectively, 15 m (the one of the raw data) and 90 m (spatial MA window length). For comparison, Fig. 3(a) and (b) also  
 104 plot the estimated SBLH from the collocated MWR, which is retrieved from the potential temperature profile [5]. On average  
 105 over the entire time interval, the estimated SBLH falls well within the MWR errorbars. In the 0-5 UTC time interval, the mean  
 106 estimated SBLH is  $510 \text{ m} \pm 300 \text{ m}$  (TVAR) and  $490 \text{ m} \pm 90 \text{ m}$ . During 21-24 UTC, the mean SBLH and uncertainty is  $450 \text{ m}$   
 107  $\pm 180 \text{ m}$  (TVAR) and  $430 \text{ m} \pm 90 \text{ m}$  (MWR).

108 The second study case (29/04/2013) is a limiting one characterised by a low aerosol load in the SBL, which causes that  
 109 height-resolved backscatter variance profiles do not yield a clear signature of the MVRs. Fig. 4 shows the backscatter plot  
 110 along with sparse SBLH estimates between 0-1:30 UTC and 4-4:30 UTC.

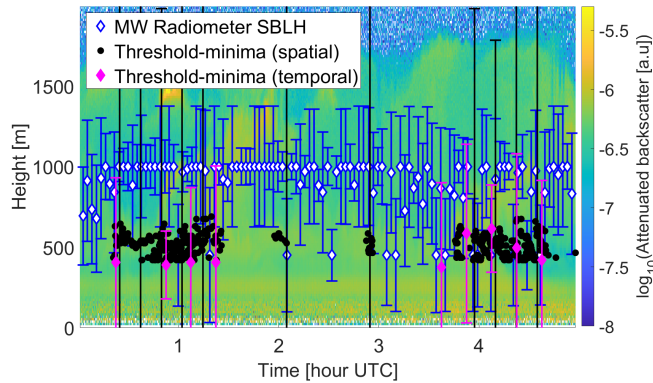


**Fig. 4.** Limiting case on SBLH estimation involving shallow mixing and lack of aerosol stratification. Early morning, 29/4/2013.

## 5. CONCLUSIONS

111

112 A simplistic method for estimating the nocturnal stable boundary layer height (SBLH) based on the identification of minimum  
 113 variance regions (MVR) using ceilometer data has been presented and applied to two test cases representative of different  
 114 atmospheric conditions. The method relies on the calculation of vertical profiles of either temporal or spatial backscatter  
 115 variance and on the application of a threshold-limited decision (TLD) criterion. When more than one MVRs are found, RS data  
 116 at a time instant within the searching interval is needed for unambiguously identifying the SBLH. The method has been applied  
 117 to data from a ceilometer. The results have been compared with SBLH estimates from a collocated MWR and demonstrate  
 118 that when no temperature profiler is available the SBLH can be successfully estimated using this method. Low aerosol optical  
 119 depths as well as the noise-induced error on the raw backscatter data limit application of the method. Further tests using a larger  
 120 amount of data need to be performed in order to quantify these error sources and their impact on the SBLH estimates.

## 6. REFERENCES

121

122 [1] T. Su, Z. Li, and R. Kahn, "A new method to retrieve the diurnal variability of planetary boundary layer height from lidar  
 123 under different thermodynamic stability conditions," *Remote Sensing of Environment*, vol. 237, p. 111519, 2020.

- 124 [2] G. Vivone et al., "Atmospheric boundary layer height estimation from aerosol lidar: a new approach based on morpho-  
125 logical image processing techniques," *Atmospheric Chemistry and Physics*, vol. 21, no. 6, pp. 4249–4265, 2021.
- 126 [3] M. Mylonaki et al., "Aerosol type classification analysis using EARLINET multiwavelength and depolarization lidar  
127 observations," *Atmospheric Chemistry and Physics*, vol. 21, no. 3, pp. 2211–2227, 2021.
- 128 [4] S. Lolli et al., "Overview of the New Version 3 NASA Micro-Pulse Lidar Network (MPLNET) Automatic Precipitation  
129 Detection Algorithm," *Remote Sensing*, vol. 12, no. 1, p. 71, 2020.
- 130 [5] R. B. Stull, "Stable Boundary Layer BT - An Introduction to Boundary Layer Meteorology," R. B. Stull, Ed. Dordrecht:  
131 Springer Netherlands, 1988, pp. 499–543.
- 132 [6] U. Saeed, F. Rocadenbosch, and S. Crewell, "Adaptive Estimation of the Stable Boundary Layer Height Using Combined  
133 Lidar and Microwave Radiometer Observations," *IEEE Trans. Geosci. Remote Sens.*, vol. 54, no. 12, pp. 6895–6906,  
134 Dec. 2016, doi: 10.1109/TGRS.2016.2586298.
- 135 [7] T. Bolling, "Ceilometer CHM 15k, NIMBUS", 2020. [https://www.lufft.com/products/cloud-height-snow-depth-sensors-  
136 288/ceilometer-chm-15k-nimbus-2300/](https://www.lufft.com/products/cloud-height-snow-depth-sensors-288/ceilometer-chm-15k-nimbus-2300/).
- 137 [8] J. G. Proakis and D. G. Manolakis, "Power Spectrum Estimation," in *Digital Signal Processing (3rd Ed.): Principles,  
138 Algorithms, and Applications*, 4th ed., USA: Prentice-Hall, Inc., 2007.
- 139 [9] R. J. Barlow, *Statistics: A Guide to the Use of Statistical Methods in the Physical Sciences*. Chichester, England: Wiley,  
140 1993.